NH_3-Assisted Ammonolysis of β-Lactams: A Theoretical Study

Natalia Díaz, Dimas Suárez, and Tomás L. Sordo*

Departamento de Química Física y Analítica, Universidad de Oviedo, Julián Clavería 8, 33006 Oviedo, Spain

Received January 26, 1999

The ring opening of 2-azetidinone via a neutral NH_3-assisted ammonolysis process is studied using different quantum chemical methods (MP2/6-31G**, B3LYP/6-31G**, and G2(MP2,SVP) levels of theory) as a first step toward the understanding of the aminolysis reaction of β-lactam antibiotics. The exploration of the corresponding potential energy surfaces renders two different mechanistic routes for the ammonolysis process catalyzed by one ammonia molecule: a concerted pathway and a stepwise one through a tetrahedral intermediate. The gas-phase activation Gibbs energies (G2(MP2,SVP) electronic energies and B3LYP/6-31G** thermal corrections) predict that the nonconcerted route is the more favored one, presenting a ΔG for the ring opening of the tetrahedral intermediate of 51.9 kcal/mol with respect to the separate reactants. This gas-phase ΔG value is 4.9 kcal/mol lower than that for the concerted process. When the MP2/6-31G** SCRF electrostatic solvation Gibbs energy is taken into account, the resultant ΔG value in solution for the stepwise rate-determining step is 55.8 kcal/mol (1.8 kcal/mol lower than the corresponding ΔG value for the concerted route). The catalytic effect of the second ammonia molecule on the stepwise mechanism amounts to 2.4 and 0.8 kcal/mol in terms of Gibbs energies in the gas phase and in solution, respectively. The rate-determining transition state has structural characteristics in accordance with the experimental interpretation of Brønsted plots for the aminolysis reaction of benzylpenicillin in which the catalytic moiety resembles an ammonium cation. Interestingly, a comparative analysis of our theoretical results for the ammonia-assisted ammonolysis of azetidinones and those previously reported for the water-assisted hydrolysis shows that the two reactions follow opposite trends regarding the energetic and structural nature of their rate-determining transition structures. The Gibbs energy profiles reported in this work may be useful as a preliminary study to understand the aminolysis reaction of β-lactam antibiotics.

Introduction

The major antigenic determinant of penicillin allergy is the penicilloyl group bound by an amide linkage to ε amino groups of lysine residues in proteins.[1] Recent experimental studies[2] of the binding of benzylpenicillin to human serum albumin (HSA) have identified benzylpenicilloyl-containing peptides in different binding regions of HSA that involve several lysine residues. Moreover, one of the bacterial enzymes inhibited by β-lactam antibiotics catalyzes a transpeptidation reaction. Thus, the reaction of ammonia and amines with β-lactam antibiotics may be of great interest to understand some of the most important chemical processes implied in the biochemical activity of those substances.

The aminolysis of the β-lactam antibiotics is a nucleophilic substitution reaction at the carbonyl of β-lactams in which an acyl group is transferred from one amino group to another, involving the C−N bond fission of the β-lactam.[1,3] Given that a proton has to be removed from the attacking amine and a proton has to be added to the leaving amino group, an important base catalysis is expected in this class of processes. On the basis of linear Gibbs energy relationships, there is kinetic evidence for a stepwise process for the general-base-catalyzed ammonolysis and aminolysis of penicillins and cephalosporins, involving the reversible formation of a tetrahedral intermediate.[1] A general mechanistic rationale of the aminolysis of β-lactams catalyzed by bases has been proposed in which, as a first step, an amine molecule attacks the carbonylic atom of the β-lactam to form a zwitterionic tetrahedral intermediate. According to this proposal, the catalysis of the reaction occurs by the formation of an encounter complex between the tetrahedral intermediate and the basic catalyst. Subsequent proton transfer from the intermediate to the catalyst would break down the intermediate to products.

In the experimental study of the aminolysis of benzylpenicillin in aqueous solutions of a series of primary monoamines and ammonia, it has been found that the importance of the different terms contributing to the observed pseudo-first-order rate constant for the disappearance of the penicillin depends on the basicity and concentration of the amine and the pH.[1,4] Particularly interesting are the kinetic terms corresponding to the uncatalyzed and amine-catalyzed aminolysis, which are the predominant terms when weakly basic amines are employed in the biologically relevant region pH 6−8. Thus, a logarithmic plot of the kinetic constant k_b for a rate dependence on $[RNH_2]^2$ against the pK_a of the

(1) (a) Page, M. I. *Acc. Chem. Res.* **1984**, *17*, 144−151. (b) Page. M. I. The mechanism of Reactions of β-lactams. In *The Chemistry of β-lactams*; Page, M. I., Ed.; Blackie Academic & Professional: London, 1992; pp 129−147.

(2) (a) Nerli, B.; Romanin, D.; Picó, G. *Chem.-Biol. Interact.* **1997**, *104*, 179−202. (b) Yvon, M.; Anglade, P.; Val, J. M. *FEBS Lett.* **1990**, *263*, 237−240. (c) Yvon, M.; Anglade, P.; Val, J. M. *FEBS Lett.* **1989**, *247*, 273−278.

(3) Georg, G. I.; Ravikumar, V. T. *The Organic Chemistry of β-Lactams*; Georg, V. T., Ed.; VCH Publishers: New York, 1993.

(4) Yamana, T.; Tsuji, A.; Miyamoto, E.; Mira, E. *J. Pharm. Pharmacol.* **1975**, *27*, 56−57.

10.1021/jo990137b CCC: $18.00
Published on Web 04/10/1999

amines is a straight line, the slope of which gives the Brønsted β-value of 1.09. The Brønsted slope β close to unity is indicative of a rate-determining transition state in which a full covalent C−N bond formation has taken place between the nucleophilic nitrogen atom and the carbonyl carbon atom of β-lactam and which carries a positive charge on either the nitrogen nucleophilic amine or on the catalytic amine molecule.

Previous theoretical works have focused on thermal and H_2O-assisted hydrolysis processes,[5] as well as alkaline hydrolysis[6] of azetidinones. More recently, the investigation of the mechanistic role of key residues in enzymes to hydrolyze peptidic bonds has also been approached by ab initio methods.[7] However, few theoretical computations have been devoted to the study of the ammonolysis and aminolysis of β-lactams.

In a previous work,[8] we have studied by means of ab initio methods the uncatalyzed ammonolysis and aminolysis of 2-azetidinone via neutral mechanisms. Analogous concerted and stepwise mechanisms have been found for both the ammonolysis and aminolysis processes, the main difference between the two reactions being only the stabilization of the transition structures owing to the greater electron-donor ability of the amine. The first mechanism corresponds to the concerted 1,2 addition of the H−NRH bond to the amide C−N bond in a syn-periplanar manner with respect to the N lone pair of 2-azetidinone. This mechanism produces the simultaneous rupture of the β-lactam ring and the transference of the H atom to the leaving amine group. The most favored mechanism is a stepwise route involving a syn tetrahedral intermediate that is formed as a result of the addition of the H−NRH bond across the carbonyl double bond of the amide with transference of the H atom to the carbonylic O atom. The syn intermediate is connected with an anti intermediate that evolves through a transition state for 1,3 hydrogen shift with simultaneous breaking of the endocyclic C−N bond to give the product 3-amino-propanamide.

From the above mechanisms, it is clear that the catalytic action of a base molecule should play an important role in the ammonolysis and aminolysis of β-lactam antibiotics. As a first approach to investigate these reactions, the neutral ammonolysis of 2-azetidinone assisted by ammonia will be studied in this work using quantum chemical methods. The electrostatic effect of solvent will be taken into account using a general self-consistent-reaction field (SCRF) model. The theoretical investigation of the NH_3-assisted ammonolysis of 2-azetidinone will provide structural and energetic data that may be useful to obtain some insight into the kinetic and thermodynamical effects of substituents of β-lactams, as well as the actual catalytic advantage of enzymatic environments on the aminolysis reaction of β-lactams.[9]

Methods

Ab initio calculations were carried out with the G94 system of programs[10] in which extra links for the solvent effect treatment have been added.[11] Stable structures were fully optimized and transition structures (TSs) were located at the HF/6-31G*, MP2/6-31G**, and B3LYP/6-31G** levels.[12,13] All the critical points were further characterized by analytic computation of harmonic frequencies at the HF/6-31G* and B3LYP/6-31G** levels. Thermodynamic data (298 K, 1 bar) were computed using B3LYP/6-31G** frequencies to obtain results more readily comparable with experiment within the ideal gas, rigid rotor, and harmonic oscillator approximations.[14] Although the preliminary HF/6-31G* results are not presented in this work, intrinsic reaction coordinate (IRC) calculations[15] at the HF/6-31G* level were carried out to confirm the reaction paths on the potential energy surface (PES) connecting the different complexes, intermediates, and products.

To estimate the effect of larger basis sets and the more elaborated *N*-electron treatments on the relative energies for the ammonolysis process, electronic energies were also computed for all of the MP2/6-31G** optimized structures using the G2(MP2,SVP) scheme,[16] which approximates the QCISD(T)/6-311+G(3df,2p) level in an additive fashion as follows:

$$E[\text{QCISD(T)/6-311+G(3df,2p)}] \approx E[\text{G2(MP2,SVP)}] = E[\text{QCISD(T)/6-31G*}] + E[\text{MP2/6-311+G(3df,2p)}] - E[\text{MP2/6-31G*}]$$

The G2(MP2,SVP) method reproduces the thermochemical data of the G2 test set with an average absolute deviation of 1.63 kcal/mol. Analogously, B3LYP/6-311+G(3df,2p) single point calculations were carried out on all the B3LYP/6-31G** optimized structures.

Quantum chemical computations on solvated structures were carried out by means of a general SCRF model[17] at the MP2/6-31G** theory level. Gas-phase MP2/6-31G** geometries were used, given that previous work on the uncatalyzed process has rendered very similar optimized geometries both in the gas phase and in solution.[8] The solvent is represented by a continuum characterized by its relative static dielectric permittivity, ϵ. The solute, which is placed in a cavity created in the continuum after spending some cavitation energy, polarizes the continuum, which in turn creates an electric field inside the cavity. Once the equilibrium is reached, the electrostatic part of the free energy corresponding to the

(5) (a) Pitarch, J.; Ruiz-López, M. F.; Silla, E.; Pascual-Ahuir, J. L.; Tuñón, I. *J. Am. Chem. Soc.* **1998**, *120*, 2146−2155. (b) Pitarch, J.; Ruiz-López, M. F, Pascual-Ahuir, J. L.; Silla, E.; Tuñón, I. *J. Phys. Chem. B*. **1997**, *101*, 3581−3588.(c) Wolfe, S. *Can. J. Chem*. **1994**, *72*, 1014−1031.

(6) (a) Frau, J.; Donoso, J.; Muñoz, F.; Vilanova, B.; García Blanco, F.; *Helv. Chim. Acta* **1997**, *80*, 739−747. (b) Frau, J.; Donoso, J.; Muñoz, F.; García Blanco, F. *Helv. Chim. Acta* **1996**, *89*, 353−361. (c) Petrongolo, G.; Ranhgino, R.; Scordamaglia, R. *Chem. Phys.* **1980**, *45*, 279−290.

(7) (a) Venturini, A.; López-Ortiz, F.; Alvarez, J. M., González, J. *J. Am. Chem. Soc.* **1998**, *120*, 1110−1111. (b) Stanton, R. V.; Perakyla, N.; Bakowies, D.; Kollman, P. A. *J. Am. Chem. Soc.* **1998**, *120*, 3448−3457. (c) Wladkowsi, B. D.; Chenoweth, S. A.; Sanders, J. N.; Kraus, M.; Stevens, W. J. *J. Am. Chem. Soc.* **1997**, *119*, 6423−6431.

(8) Díaz, N.; Suárez, D.; Sordo. T. L. *Eur. J. Chem.*, in press.

(9) Warshel, A. *Computer Modeling of Chemical Reactions in Enzymes and Solutions*; John Wiley & Sons: New York, 1991.

(10) Frisch, M. J.; Trucks, G. W.; Schlegel, H. B.; Gill, P. M. W.; Johnson, P. M. W.; Robb, M. A.; Cheeseman, J. R.; Keith, T.; Petersson, G. A.; Montgomery, J. A.; Raghavachari, K.; Al-Laham, M. A.; Zakrzewski, V. G.; Ortiz, J. V.; Foresman, J. B.; Peng, C. Y.; Ayala, P. Y.; Chen, W.; Wong, M. W.; Andres, J. L.; Replogle, E. S.; Gomperts, R.; Martin, R. L.; Fox, D. J.; Binkley, J. S.; Defrees, D. J.; Baker, J.; Stewart, J. P.; Head-Gordon, M.; Gonzalez, C.; Pople, J. A. *Gaussian 94;* Gaussian, Inc.: Pittsburgh, PA, 1995.

(11) Adapted by D. Rinaldi from Rinaldi, D.; Pappalardo, R. R. Quantum Chemistry Program Exchange, program 622; Indiana University, Bloomington, IN, 1992.

(12) Hehre, W. J.; Radom, L.; Pople, J. A.; Schleyer, P. v. R. *Ab Initio Molecular Orbital Theory*; John Wiley & Sons Inc.: New York, 1986.

(13) (a) Becke, A. D. *J. Chem. Phys.* **1993**, *98*, 5648−5652. (b) Becke, A. D. *Phys. Rev. A.* **1988**, *38*, 3098−3100. (c) Lee, C.; Yang, W.; Parr, R. G. *Phys. Rev. B.* **1988**, *37*, 785−789.

(14) McQuarrie, D. A. *Statistical Mechanics*; Harper & Row: New York, 1976.

(15) (a) Fukui, K. *Acc. Chem. Res.* **1981**, *14*, 363. (b) González, C.; Schlegel, H. B. *J. Phys. Chem*. **1990**, *94*, 5523.

(16) Curtiss, L. A.; Redfem, P. C. Smith, B. J.; Radom, L. *J. Chem. Phys*. **1996**, *104*, 5148.

(17) (a) Rivail, J. L.; Rinaldi, D.; Ruiz-López, M. F. In *Theoretical and Computational Model for Organic Chemistry*; Formosinho, S. J., Csizmadia, I. G., Arnaut, L., Eds.; Kluwer Academic Publishers: Dordrecht, 1991; NATO ASI Series C, Vol. 339, pp 79−92. (b) Dillet, V.; Rinaldi, D.; Angyán, J. G.; Rivail, J. L. *Chem. Phys. Lett.* **1993**, *202*, 18. (c) Dillet, V.; Rinaldi, D.; Rivail, J. L. *J. Phys. Chem*. **1994**, *98*, 5034−5039.

Scheme 1

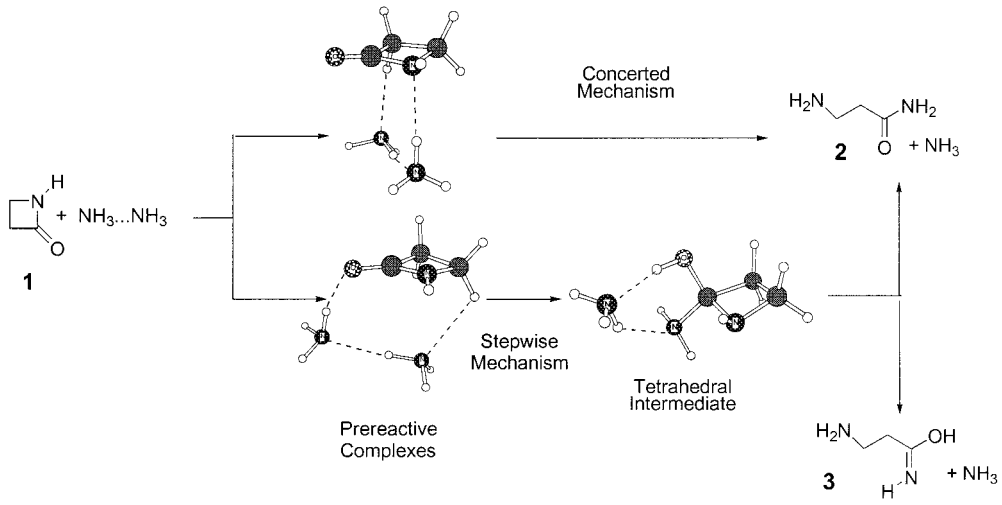

solvation process is obtained using a monocentric multipolar expansion of the molecular charge distribution.[18] The SCRF continuum model employed assumes a general cavity shape that is obtained using van der Waals solute atomic spheres with modified radii ($1.3084 \cdot r_{vdW}$),[17a] necessary to fulfill the volume condition. A relative permittivity of 78.30 was used to simulate water as the solvent used in the experimental work.

The main TSs were also analyzed carrying out a configurational analysis (CA).[19] This interpretative tool rewrites a TSs monodeterminantal wave function (built in this work from the B3LYP/6-31G** MOs) as a combination of the electronic configurations of the interacting fragments, thus obtaining a more chemically graspable picture. This analysis was performed using a revised version of the ANACAL program.[20]

Results and Discussion

An extensive exploration of the PESs at the different theory levels used in this work was carried out for the neutral ammonolysis of 2-azetidinone catalyzed by one ammonia molecule, rendering two possible pathways for this process (see Scheme 1).

These pathways correspond to a concerted and a stepwise mechanism for the ring opening of β-lactam passing through the respective initial prereactive complexes between 2-azetidinone and the ammonia dimer.[21] The first mechanism consists of the concerted nucleophilic attack of the NH_3 fragment to the amide C atom by one of the NH_3 components of the ammonia dimer from which a proton is removed by the second NH_3 moiety, from which in turn a proton is transferred to the leaving amine group with the simultaneous rupture of the β-lactam ring **1**. The stepwise mechanism proceeds through the NH_3-assisted addition of the $H-NH_2$ bond across the carbonyl double bond to give an amino-alcohol tetrahedral intermediate. The ring opening of this intermediate can take place through the proton transference from the hydroxyl group to the endocyclic nitrogen facilitated by the catalytic NH_3 molecule, leading to the final propanamide product **2** (see Scheme 1). We also studied another alternative for the evolution of the tetrahedral intermediate, consisting of the NH_3-catalyzed proton transference from the amino group to the amidic N atom to give an open-chain hydroxy-imine product **3**. As we will see later, the formation of **3** is clearly disfavored both kinetically and thermodynamically with respect to the formation of **2**.

The optimized geometries of the structures located along the concerted and stepwise reaction paths for the gas-phase reaction of 2-azetidinone with the ammonia dimer are shown in Figure 1. Table 1 collects the relative energies along the reaction profiles obtained at the different theory levels including the ZPVE correction from the B3LYP/6-31G** unscaled frequencies.

We will present and discuss first the structural and energetic results for the concerted mechanism and then those corresponding to the stepwise route. The effect of high-level theoretical methods, thermodynamical analysis, and the electrostatic influence of solvent will be subsequently addressed.

Concerted Mechanism. The first critical structure located along the concerted reaction path for the catalyzed ammonolysis of 2-azetidinone is an intermolecular complex between the ammonia dimer and 2-azetidinone ($\mathbf{C_c}$ in Figure 1). In this complex, the ammonia dimer is located parallel to the β-lactam ring. The catalytic NH_3 molecule acts as an acceptor end in a H-bond interaction with the amidic center (NH···N $\approx$ 2.3 Å) while the nucleophilic NH_3 molecule establishes a weak CH···N bond with one of the methylene groups of 2-azetidinone (CH···N $\approx$ 2.3 Å). The H bond between NH_3 and the amidic center causes a partial loss of the amidic resonance as reflected in the pyramidalization of the N atom (the sum of the CNH and CNC angles is ~348 degrees). MP2/6-31G** and B3LYP/6-31G** levels of theory predict similar binding energies of −7.8 and −6.4 kcal/mol for the $\mathbf{C_c}$ structure.

According to IRC calculations, the nucleophilic attack of the NH_3 molecule to the carbonylic C atom of 2-azetidinone leads from $\mathbf{C_c}$ to a TS for the concerted ammonolysis process of 2-azetidinone ($\mathbf{TS_c}$ in Figure 1). $\mathbf{TS_c}$ presents a very tight structure with a single C(azetidi-

(18) Claverie, P. In *Quantum Theory of Chemical Reactions*; Daudel, R., Pullman, A., Salem, L., Veillard, A., Eds.; Reidel: Dordrecht, 1982; Vol. 3, pp 151−175.

(19) (a) Fujimoto, H.; Kato, S.; Yamabe, S.; Fukui, K. *J. Chem. Phys.* **1974**, *60*, 572. (b) Menéndez, M. I.; Sordo, J. A.; Sordo, T. L *J. Phys. Chem.* **1992**, *96*, 1185−1187.

(20) López, R.; Menéndez, M. I.; Suárez, D.; Sordo, T. L.; Sordo, J. A. *Comput. Phys. Commun.* **1993**, *76*, 235−249.

(21) MP2/6-31G** and B3LYP/6-31G** levels of theory render a similar structure (N···N ≈ 3.2 Å) and interaction energies for the linear ammonia dimer (−4.2 and −4.3 kcal/mol, respectively) in agreement with previous theoretical data: (a) Tao, F.; Klemperer, W. *J. Chem. Phys.* **1993**, *99*, 5976−5982. (b) Kieninger, M.; Suhai, S. *J. Comput. Chem.* **1996**, *17*, 1508−1519.

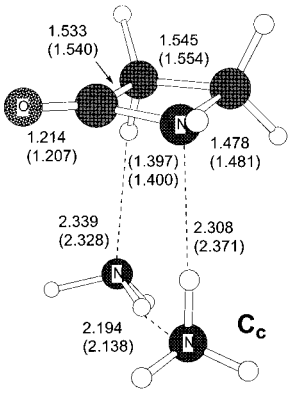

C_c

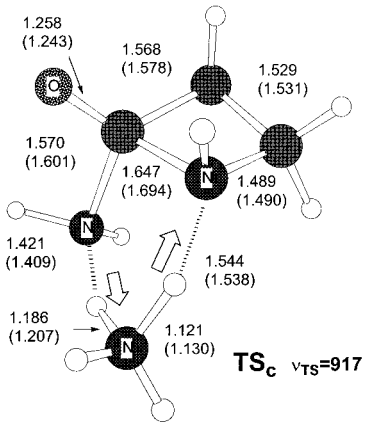

TS_c ν_{TS}=917 i cm^{-1}

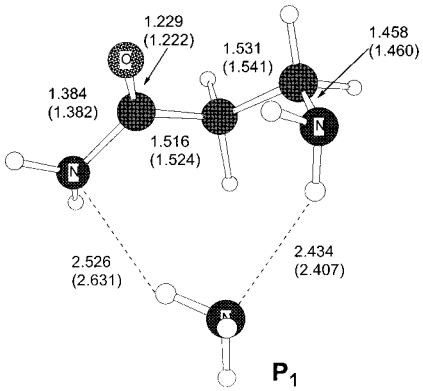

P_1

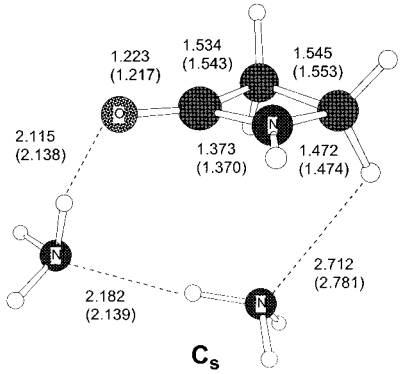

C_s

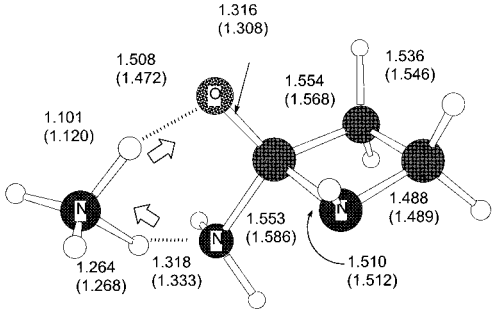

TS_1 ν_{TS}=1210 i cm^{-1}

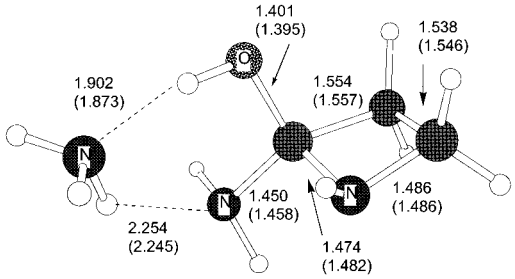

I_1

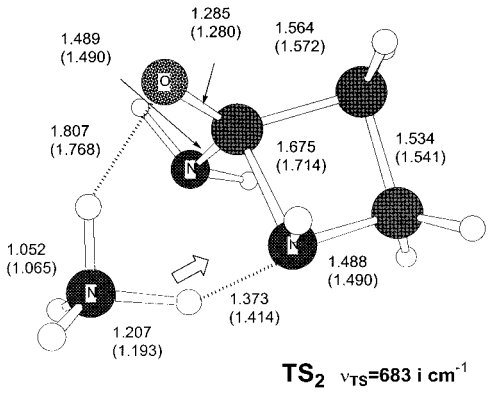

TS_2 ν_{TS}=683 i cm^{-1}

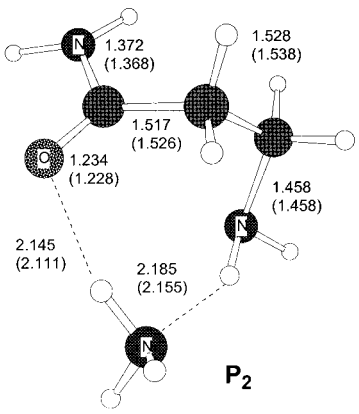

P_2

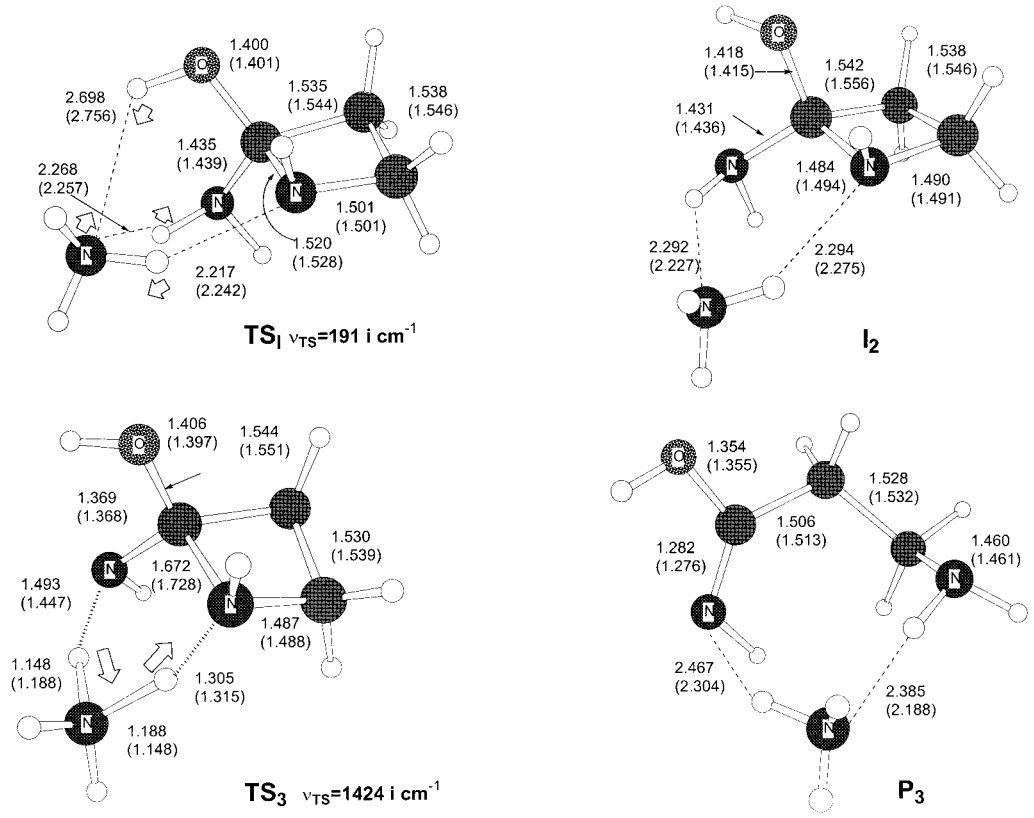

Figure 1. MP2/6-31G** optimized structures for the NH_3-assisted ammonolysis reaction of 2-azetidinone. Distances are in Å. B3LYP/6-31G** values are in parentheses. At TSs, hollow arrows sketch the main components of the corresponding transition vectors.

Table 1. Relative Energies[a] (kcal/mol) with Respect to Reactants of the Structures Considered in the NH_3-Assisted Ammonolysis of 2-Azetidinone

structures	MP2/6-31G**	MP2/6-31G** SCRF $\epsilon = 78.3$[b]	G2(MP2,SVP)	B3LYP/6-31G**	B3LYP/ 6-311+G(3df,2p)[c]
$NH_3 + NH_3$+ 2-azetidinone	0.0	0.0 (−12.2)	0.0	0.0	0.0
C$_c$	−7.8	−4.8 (−9.1)	−5.0	−6.4	−1.5
TS$_c$	29.0	29.8 (−11.4)	35.7	29.8	40.4
P$_1$	−24.0	−20.0 (−6.5)	−20.9	−21.4	−15.4
$NH_3 + H_2N(CH_2)_2CONH_2$	−21.9	−19.5 (−6.2)	−20.0	−20.6	−17.2
C$_s$	−10.9	−3.4 (−4.6)	−8.1	−9.8	−4.2
TS$_1$	22.3	25.5 (−9.0)	27.9	24.2	34.6
I$_1$	−1.2	6.0 (−4.9)	1.9	4.1	12.3
TS$_2$	26.0	29.9 (−8.3)	30.2	30.5	40.3
P$_2$	−25.7	−19.4 (−5.9)	−22.4	−23.0	−16.0
TS$_I$	6.1	13.5 (−4.7)	7.1	11.2	18.5
I$_2$	3.1	11.1 (−4.1)	5.2	8.0	15.4
TS$_3$	34.0	40.6 (−5.6)	37.9	35.1	45.9
P$_3$	−9.2	−2.7 (−5.4)	−8.3	−9.0	−3.7
$NH_3 + H_2N(CH_2)_2C(OH)NH$	−4.7	−1.7 (−5.6)	−5.2	−2.5	−0.6

[a] Including ZPVE corrections from the B3LYP/6-31G** frequencies. [b] Single point calculations on gas-phase MP2/6-31G** geometries. Solvation Gibbs energies (kcal/mol) are in parentheses. [c] Single point calculations on gas-phase B3LYP/6-31G** geometries.

none)−N(NH_3) bond practically formed, whereas the endocyclic C−N bond is barely cleft (both the forming and the breaking C−N bond lengths are around 1.6 Å). The B3LYP/6-31G** transition vector at **TS$_c$** consists basically of the transference of a H atom from the nucleophilic NH_3 molecule to the catalytic NH_3 molecule and the simultaneous transference of another H atom from the catalyst to the ring N atom. The MP2/6-31G** energy barrier corresponding to this concerted TS is 36.8 kcal/mol with respect to the initial **C$_c$** complex (very close to the B3LYP/6-31G** value, 36.2 kcal/mol). Comparing the MP2/6-31G** value with that corresponding to the noncatalyzed ammonolysis reaction (47.6 kcal/mol),[8] we see that the energy barrier decreases by 10.8 kcal/mol as a result of the catalytic action of the second ammonia molecule.

An examination of the IRC reaction coordinate along the product channel reveals that, after passing **TS$_c$**, the hydrogen shift is completed and then the ring opening of β-lactam proceeds through the elongation of the breaking C−N bond to form a product complex **P$_1$** (see Figure 1). **P$_1$** is 24.0 and 21.4 kcal/mol more stable than separate reactants at the MP2/6-31G** and B3LYP/6-31G** levels, respectively. As expected, these values predict an important thermodynamic driving force for the ammonolysis reaction. IRC calculations confirm that

most of this exoergicity results from the release of the strain energy of the four-membered ring at the latter stages of the reaction coordinate.[8] In $\mathbf{P_1}$ the 3-amino-propanamide is bonded to the catalytic NH_3 molecule through two intermolecular H bonds in which amide and amino groups in 3-amino-propanamide act as donor (N···HN ≈ 2.5 Å) and acceptor (NH···N ≈ 2.4 Å) groups, respectively. Dissociation of this product complex $\mathbf{P_1}$ into the separate products, NH_3 + 3-propanamide, requires 2.1 kcal/mol at MP2/6-31G** level (0.8 kcal/mol at B3LYP/6-31G**). These binding energies are given with respect to the most stable conformer of 3-aminopropanamide that presents an intramolecular H bond between the amino and amide groups.[8]

Stepwise Mechanism: Formation of the Tetrahedral Intermediate. Concerning the stepwise mechanism for the catalyzed ammonolysis of 2-azetidinone, the first critical structure located along the reaction coordinate is also a prereactive complex between the ammonia dimer and the β-lactam ($\mathbf{C_s}$ in Figure 1). The ammonia dimer is located parallel to the β-lactam, with the nucleophilic NH_3 molecule situated above the middle point of the β-lactam ring presenting a weak H-bonding interaction with one of the methylene groups of 2-azetidinone (see Figure 1). The catalytic NH_3 molecule forms a typical O···HN H bond with the carbonylic oxygen atom, having an equilibrium distance of around 2.1 Å. It is interesting to note that in the $\mathbf{C_s}$ prereactive complex, the N ring atom presents a slight pyramidalization, determining an antiperiplanar orientation of its lone pair with respect to the nucleophilic lone pair of the attacking ammonia.

$\mathbf{C_s}$ evolves through a TS for the addition of one ammonia N−H bond across the C−O double bond of 2-azetidinone ($\mathbf{TS_1}$ in Figure 1). The IRC calculation connecting $\mathbf{C_s}$ and $\mathbf{TS_1}$ reveals that along the reactant channel the reaction coordinate involves initially a ring-puckering motion of 2-azetidinone, followed by the nucleophilic attack of NH_3 and the simultaneous out-of-plane bending motion of the N−H bond in 2-azetidinone. This latter motion leads to a synperiplanar orientation of the attacking NH_3 molecule with respect to the N lone pair of 2-azetidinone (see Figure 1).[22] The forming C−N bond is quite advanced at $\mathbf{TS_1}$ (∼1.55 Å), the B3LYP/6-31G** transition vector being clearly dominated by the proton shifts sketched in Figure 1. The calculated energy barriers with respect to the initial complex for $\mathbf{TS_1}$ are 33.2 and 34.0 kcal/mol at the MP2/6-31G** and B3LYP/6-31G** levels, respectively. The catalytic effect of the second NH_3 molecule is then 14.9 and 15.1 kcal/mol at the MP2/6-31G** and B3LYP/6-31G** levels, respectively,[8] about 4 kcal/mol greater than for the concerted TS.

The IRC pathway leads from $\mathbf{TS_1}$ to a stable intermediate $\mathbf{I_1}$ in which the four-membered ring is not planar given that the carbonylic C atom becomes a tetrahedral center. The catalytic NH_3 molecule is linked to this intermediate by two strong H bonds: OH···N (∼1.9 Å) and N···HN (∼2.2 Å) interactions (see Figure 1) in which hydroxy and amino groups of the intermediate act as acceptor and donor ends, respectively. These H bonds stabilize the $\mathbf{I_1}$ complex by 11.3 kcal/mol at the MP2/6-31G** level (10.4 kcal/mol at B3LYP/6-31G**). Nevertheless, $\mathbf{I_1}$ remains less stable than its precursor complex $\mathbf{C_s}$ by 6.7 kcal/mol (MP2/6-31G**) or 11.7 kcal/mol (B3LYP/6-31G**).

Stepwise Mechanism: Evolution of the Tetrahedral Intermediate. The ring opening of the intermediate $\mathbf{I_1}$ takes place through the $\mathbf{TS_2}$ transition structure (see Figure 1). The analysis of an IRC calculation reveals the following chemical events along the reaction coordinate from $\mathbf{I_1}$ to $\mathbf{TS_2}$: first, the H-transference from the hydroxyl group to the catalytic NH_3 molecule gives rise to an ammonium group, and second, this NH_4^+ fragment moves along an out-of-plane bending motion with respect to the β-lactam ring. In this way, $\mathbf{TS_2}$ is reached where a H atom is being transferred from the NH_4^+ moiety to the leaving amino group with simultaneous partial breaking of the endocyclic C−N bond (∼1.7 Å). The energy barriers corresponding to $\mathbf{TS_2}$ with respect to $\mathbf{C_s}$ are 36.9 and 40.3 kcal/mol at the MP2/6-31G** and B3LYP/6-31G** levels, respectively. Thus, $\mathbf{TS_2}$ is the kinetic controlling TS in the stepwise mechanism for the catalyzed ammonolysis of 2-azetidinone (see Table 1). It is also interesting to note that although the MP2 and B3LYP geometries of $\mathbf{TS_2}$ are quite similar, the corresponding energy barriers present the most remarkable difference found in this work. Therefore, according to the MP2/6-31G** and B3LYP/6-31G** energy barriers computed in this work, the concerted mechanism is the most favored one by 0.1 kcal/mol (MP2/6-31G**) and 3.4 kcal/mol (B3LYP/6-31G**), in contrast with the experimental evidence (see below for a high-level energy profile).

The C−N bond in $\mathbf{TS_2}$ completely breaks during the subsequent evolution of the reaction coordinate by a stretching motion that releases a major part of the strain energy of 2-azetidinone, which amounts to 28.9 kcal/mol at the MP2/6-31G** level without including ZPVE correction (this strain energy was computed through the corresponding homodesmic reaction).[8] According to the analysis of the IRC energy profile,[8] this release of strain energy takes place in the last stages of the ring-opening process and has only very moderate kinetic influence. The ring opening of $\mathbf{TS_2}$ gives a very stable product complex, $\mathbf{P_2}$, which is 25.7 and 23.0 kcal/mol more stable than isolated reactants at the MP2/6-31G** and B3LYP/6-31G** levels, respectively. This product complex dissociates into the separate products, which are 3.8 kcal/mol (MP2/6-31G**) and 2.4 kcal/mol (B3LYP/6-31G**) above it. From data in Figure 1 and Table 1, we see that $\mathbf{P_2}$ and $\mathbf{P_1}$ differ in the nature of the H bonds between 3-amino-propanamide and the catalytic NH_3 molecule, the $\mathbf{P_2}$ conformer being around 2.0 kcal/mol more stable than $\mathbf{P_1}$.

Figure 1 shows a second tetrahedral intermediate $\mathbf{I_2}$ that is connected with the intermediate $\mathbf{I_1}$ through the transition state $\mathbf{TS_I}$ (see Figure 1) with an energy barrier of about 7 kcal/mol with respect to $\mathbf{I_1}$ and a transition vector that implies the simultaneous breaking and forming of intermolecular H bonds. At the MP2/6-31G** and B3LYP/6-31G** levels, $\mathbf{I_2}$ is 4.8 and 4.4 kcal/mol, respectively, less stable than $\mathbf{I_1}$. The IRC reaction path shows that $\mathbf{I_2}$ evolves through a TS ($\mathbf{TS_3}$ in Figure 1) for the simultaneous cleavage of the endocylic C−N bond and the NH_3-assisted proton transfer from the exocyclic amino group in the tetrahedral intermediate $\mathbf{I_2}$ to the

(22) In contrast with the noncatalyzed process, an antiperiplanar stereoisomer of this TS could not be found on the PES. Nevertheless, the synperiplanar orientation can be well understood in terms of the greater weight of the $NH_3 \rightarrow$ 2-azetidinone charge transfer in the syn orientation than in the anti one (see ref 8). This circumstance could have consequences for the placement of catalytic groups in a protein environment.

forming amino group, rendering a hydroxy-imine product complex (**P_3** in Figure 1). Although the geometrical structure and the transition vector of **TS_3** are comparable with those of the previously discussed TSs, **TS_3** is the least stable one, 8.0 and 4.6 kcal/mol above **TS_2** at the MP2/6-31G** and B3LYP/6-31G** levels, respectively. This alternative mechanism for the evolution of the tetrahedral intermediate is also thermodynamically noncompetitive given that **P_3** is clearly less stable than **P_2** by 16.5 and 14.0 kcal/mol at the MP2/6-31G** and B3LYP/6-31G** levels, respectively (see Table 1). Dissociation of this product complex **P_3** into the separate products requires 4.5 kcal/mol at the MP2/6-31G** level (6.5 kcal/mol at B3LYP/6-31G**).

High-Level Energy Profiles. Both correlated methods used in this work (MP2/6-31G** and B3LYP/6-31G**) provide similar geometries for the initial complexes, intermediates, and TSs located along the reaction coordinate. The corresponding relative energies collected in Table 1 show that the MP2 and B3LYP energy profiles are quite comparable for the prereactive complexes, **TS_c**, **TS_1**, and **TS_3** structures, whereas the rest of the B3LYP/6-31G** energy profile is less stable than the MP2 profile by 4−5 kcal/mol.

As already mentioned, at the MP2/6-31G** and B3LYP/6-31G** levels the concerted mechanism is more favorable than the stepwise one by only 0.1 and 4.1 kcal/mol, respectively. In view of the experimental evidence in favor of a stepwise process and the small energy differences between **TS_c** and **TS_2,** particularly at the MP2/6-31G** level, we have further investigated the energy profiles at higher levels of theory.

First, the effect of a larger basis set on the energy profiles was investigated by means of single-point calculations at the B3LYP/6-311+G(3df,2p)//B3LYP/6-31G** level. In general, an appreciable raise of 9 or 10 kcal/mol in all the relative energies is observed, although none of the above-discussed trends along the B3LYP/6-31G** reaction profile become modified and the concerted mechanism remains the most favorable one by 2.6 kcal/mol.

When improving both the basis set and the N-electron treatment using the G2(MP2,SVP) procedure, the resultant relative energies are about 4−5 kcal/mol above the MP2/6-31G** values (see Table 1). At the G2(MP2,SVP) level, the stepwise mechanism becomes the most favorable one. **TS_2,** which remains the rate-determining TS in the nonconcerted mechanism, has an energy barrier of 38.3 kcal/mol, which is 2.4 kcal/mol lower than that of **TS_c**. Thus, the inclusion of high-level corrections is crucial to estimate the kinetic preference between the stepwise and concerted mechanisms and favors the stepwise one. It may also be interesting to compare the relative energies of the TSs. The G2(MP2,SVP) calculations predict that **TS_1** is 2.4 kcal/mol more stable than **TS_2**, whereas **TS_c** is 5.5 kcal/mol less stable than **TS_2**. At the MP2/6-31G** and B3LYP/6-31G** levels, **TS_2** presents a relative energy of −3.0 and 0.7 kcal/mol, respectively, with respect to **TS_c**, while **TS_1** is in turn 3.7 and 6.3 kcal/mol more stable than **TS_2**. Therefore, the MP2/6-31G** relative energies of the main TSs are closer to the G2(MP2,SVP) values than the B3LYP/6-31G** results. The G2(MP2,SVP) high-level corrections also tend to stabilize the stepwise product complex with respect to the concerted one given that the **P_1** and **P_2** product complexes are now 20.9 and 22.4 kcal/mol more stable than the separate reactants, respectively. The separate products are 20.0 kcal/mol below the initial separate reactants (see Table 1).

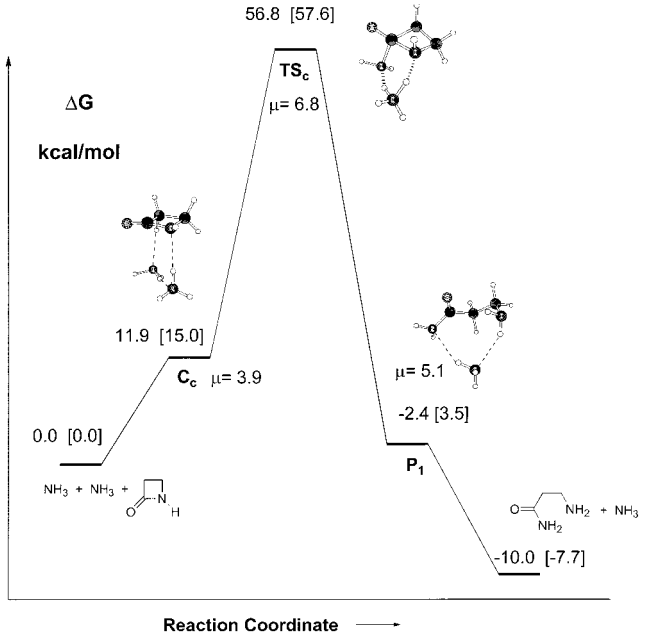

Figure 2. Gibbs energy profiles (kcal/mol) both in the gas phase and in solution (in brackets) for the concerted reaction channel corresponding to the NH_3-assisted ammonolysis reaction of 2-azetidinone. Thermal corrections to Gibbs energies were computed using the B3LYP/6-31G** analytical frequencies, and electronic energies and solvation Gibbs energies were calculated at the G2(MP2,SVP) and MP2/6-31G** SCRF levels, respectively. Gas-phase MP2/6-31G** dipole moments (in debyes) are also displayed.

Gibbs Energy Profiles in Gas Phase and in Solution. The relative Gibbs energy values with respect to the separate reactants are given in Figures 2 and 3 for the concerted and stepwise mechanisms for the NH_3-assisted ammonolysis reaction of 2-azetidinone, respectively, both in the gas phase and in solution. The gas-phase ΔG values combine the G2(MP2,SVP) electronic energies and the thermal corrections from the B3LYP/6-31G** analytical frequencies. The electrostatic contribution to the solvation Gibbs energy was calculated by means of MP2/6-31G** SCRF (ϵ = 78.3) single-point calculations on the MP2/6-31G** gas-phase geometries. Of course, a more active participation of solvent molecules in the reaction than modeled by our continuum SCRF calculations is to be expected. Table 1 contains the MP2/6-31G** SCRF relative energies and solvation Gibbs energies for all of the structures considered in this work.

When thermal corrections to the G2(MP2,SVP) gas-phase 0 K energies are included, both the prereactive complexes and product complexes are no longer stable with respect to the separate reactants and products, respectively. Thus, the ΔG for the formation of the **C_c** and **C_s** prereactive complexes are 11.9 and 8.5 kcal/mol, respectively, whereas **P_1** and **P_2** are 7.6 and 6.8 kcal/mol less stable than the separate products. The ΔG_{rxn} is −10.0 kcal/mol. The calculated gas-phase activation Gibbs energies predict that the nonconcerted route is the most favored one, presenting a ΔG of 51.9 kcal/mol for the rate-determining **TS_2** which is 29.6 kcal/mol above the intermediate **I_1**. The ΔG barrier corresponding to the concerted process is 56.8 kcal/mol, 4.9 kcal/mol higher than the nonconcerted one. For the noncatalyzed ammonolysis

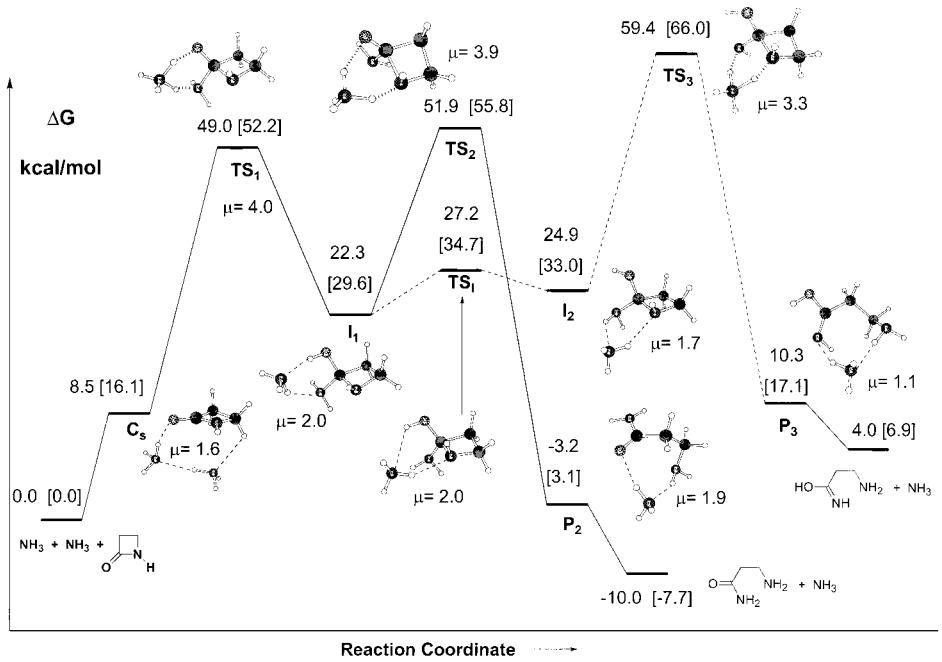

Figure 3. Gibbs energy profiles (kcal/mol) both in the gas phase and in solution (in brackets) for the stepwise reaction channel corresponding to the NH_3-assisted ammonolysis reaction of 2-azetidinone. Thermal corrections to Gibbs energies were computed using the B3LYP/6-31G** analytical frequencies, and electronic energies and solvation Gibbs energies were calculated at the G2(MP2,SVP) and MP2/6-31G** SCRF levels, respectively. Gas-phase MP2/6-31G** dipole moments (in Debyes) are also displayed.

we found a ΔG barrier of 56.7 and 54.7 kcal/mol for the concerted and stepwise mechanisms. Therefore, the catalytic effect of the second ammonia molecule in terms of gas-phase Gibbs energies is practically null for the concerted route, whereas for the stepwise mechanism it amounts to 2.4 kcal/mol.

When the electrostatic effect of solvent is included using a continuum model, the calculated solvation Gibbs energies for all of the critical structures correlate reasonably well with the MP2/6-31G** dipolar moments displayed in Figures 2 and 3. In general, the MP2/6-31G** SCRF ($\epsilon = 78.3$) solvation Gibbs energy is greater in absolute value for the separate reactants than for the critical structures located along the different mechanisms by 3−8 kcal/mol, with the exception of **TS$_c$** (see Table 1). The solvation Gibbs energies of **TS$_1$** and **TS$_2$** are less than 4 kcal/mol lower in absolute value than that of reactants, and the corresponding value for **TS$_c$**, which presents the largest dipole moment, amounts to −11.4 kcal/mol, only 0.7 kcal/mol lower in absolute value than that for reactants.

Solvent stabilizes in a preferential manner the TS for the concerted mechanism given that, in contrast with the rest of TSs, **TS$_c$** presents a bare accumulation of charge in the oxygen atom, capable of polarizing the solvent continuum to a larger extent. At the MP2/6-31G** SCRF level, the solvation Gibbs energy of **TS$_c$** is 3.1 kcal/mol greater in absolute value than that of the rate-determining TS of the stepwise mechanism, **TS$_2$** (see Table 1). Nevertheless, when solvation Gibbs energies are added to the gas-phase values, **TS$_2$** is 1.8 kcal/mol more stable than **TS$_c$** and presents a ΔG in solution of 55.8 kcal/mol. The electrostatic effect of solvent increases the catalytic effect in the case of the concerted mechanism (1.2 kcal/mol), whereas it diminishes that for the stepwise route (0.8 kcal/mol). Although a direct comparison between our theoretical results and experimental data is not feasible, the magnitude of the calculated activation Gibbs energy for NH_3-assisted ammonolysis of 2-azetidinone (55.8 kcal/mol) is consistent with the experimental fact that the direct reaction at 35 °C of benzylpenicillin with amines having a pK_a around 10−11 is extremely slow in the neutral pH region (half-lives are of the order of 100−400 h).[4]

It is interesting to compare our results with those obtained very recently by Pitarch et al.[5a] at the MP2/6-31G*//HF/6-31G* SCRF level for the neutral hydrolysis of *N*-methylazetidinone catalyzed by water. The ΔG energy barriers for hydrolysis are roughly 5 kcal/mol lower than those for ammonolysis. Moreover, unlike in the ammonolysis reaction, the rate-determining step for the hydrolysis stepwise mechanism corresponds to the initial nucleophilic attack of water, which presents an energy barrier 10 kcal/mol greater than that for the second step in which the tetrahedral intermediate evolves into the products. Most importantly, in the case of the hydrolysis the concerted mechanism is the most favored one by 2 kcal/mol.

Analysis of the Transition Structures. From the data discussed above, it can be noted that **TS$_c$**, **TS$_1$**, **TS$_2$**, and **TS$_3$** have several structural characteristics in common. Thus, the C−N single bond between the nucleophilic NH_3 molecule and the carbonylic C atom in 2-azetidinone is practically formed, with bond lengths in the range of 1.35−1.55 Å. Analogously, the endocyclic C−N bond is barely opened in these TSs (C−N bond distances range from 1.51 to 1.68 Å) while the ammonia-assisted proton transference to the forming hydroxyl (**TS$_1$**) or amino (**TS$_c$**, **TS$_2$**, and **TS$_3$**) groups is far from being completed (see Figure 1). In fact, the two H atoms involved in the proton transference are preferentially bonded to the catalytic N atom. In effect, a B3LYP/6-31G** configurational analysis[19] of the **TS$_c$** and **TS$_1$** structures clearly shows that these TSs can be best considered as A−B systems composed of two fragments, A = NH_4^+ and B = 1,1-amino-alcohoxy anion, interacting

with each other.[23] This is in agreement with the experimental evidence obtained through the Brønsted plot for the aminolysis of benzylpenicillin in aqueous solutions that a positive charge is developed in the catalyst at the rate-determining TS (**TS_2** according to our results). In fact, our analysis shows that a NH_4^+ moiety can be clearly distinguished in all of the TSs, interacting with a 1,1-amino-alcoholate anion in **TS_c**, **TS_1** and **TS_2** or with a 1,1-hydroxy-imine anion in **TS_3**.

The characterization of two interacting ionic moieties in these TSs allows us to understand in a qualitative manner their relative stability. On one hand, the partial localization of a negative charge on the more electronegative oxygen atom instead of a nitrogen atom results in a 1,1-amino-alcoholate anion that is 17.0 and 16.4 kcal/mol, respectively, more stable than the isoelectronic 1,1-hydroxy-imine anion at the MP2/6-31G** and B3LYP/6-31G** levels. Therefore, the lower stability of **TS_3** compared with **TS_2** seems to stem in great measure from the relative instability of the 1,1-hydroxy-imine anionic moiety with respect to the 1,1-amino-alcoholate anion. On the other hand, the MP2/6-31G** electrostatic potentials exerted by the 1,1-amino-alcoholate moieties on the center of mass of the ammonium cation in **TS_1**, **TS_2**, and **TS_c** (−137.3, −137.0, and −129.7 kcal/mol) correlate reasonably well with the relative energies of these TSs (0.0, 3.7, and 7.8 kcal/mol). The calculation of the corresponding MP2/6-31G** dipole moments (4.0, 3.9, and 6.8 D) also supports the hypothesis of a charge control on the relative stabilities of these TSs. As previously mentioned, at **TS_c** the oxygen atom carries a negative charge which is not compensated by a direct contact with the NH_4^+ moiety, rendering thus a higher dipolar moment, a lower gas-phase stability, and a lower electrostatic interaction with NH_4^+ than those of **TS_1** and **TS_2**. Therefore, electrostatic factors governing the interaction between the ammonium and the amino-alcoholate moieties seem to control the relative stability of the TSs involved in the concerted and stepwise mechanisms of the neutral ammonolysis of 2-azetidinone.

Interestingly, the rate-determining TSs for the H_2O-assisted hydrolysis of *N*-methylazetidinone studied by Pitarch et al.[5a] present important differences with respect to their corresponding counterparts in ammonolysis. Thus, at **TS_c** and **TS_1** structures for the hydrolysis reaction, the proton transference from the catalytic H_2O molecule to azetidinone is completed while the C−O forming bond remains in an initial stage. The structural comparison between the hydrolysis and ammonolysis reaction profiles reveals that in general the main TSs for hydrolysis present an opposite charge displacement with respect to the ammonolysis TSs, with the catalytic H_2O resembling a hydroxyl anion. These electronic and structural differences are in consonance with the previously discussed Gibbs energy profiles for the hydrolysis and ammonolysis reactions.

(23) The B3LYP/6-31G** configurational analyses were carried out assuming two different fragment partitions. The coefficient of the zero-configuration AB, in both **TS_c** and **TS_1**, has a much greater value ($C_{AB} \approx 0.65$) when A = NH_4^+ and B = 1,1-amino-alcohoxy anion than in the case of assuming an A = $(NH_3)_2$ and B = 2-azetidinone fragment interaction ($C_{AB} \approx 0.42$). Similarly, the electronic structures of **TS_2** and **TS_3** are dominated by the corresponding ionic partition with zero configuration values of $C_{AB} \approx 0.68$ and 0.58, respectively. Therefore, neither *reactant-like* nor *product-like* configurations dominate the electronic structure of these TSs for NH_3-assisted proton transference processes.

Conclusions

High-level theoretical calculations, including the electrostatic effect of solvent, on the reaction of 2-azetidinone with the ammonia dimer via neutral mechanisms render structural and energetic data that are compatible with experimental evidences on the aminolysis and ammonolysis of benzylpenicillin, rendering thus further understanding of the mechanism of the aminolysis of β-lactams. The reaction is theoretically predicted to proceed in a stepwise manner through a non-zwitterionic tetrahedral intermediate that is less stable than reactants and the prereactive complex. The calculated activation Gibbs energies in solution predict that the NH_3-assisted cleavage of the intermediate constitutes the kinetic-controlling step of the stepwise mechanism. The corresponding activation Gibbs energy is 39.7 kcal/mol with respect to the prereactive complex, which is consistent with the slow kinetics for the reaction of benzylpenicillin with monoamines.

The details of the electronic and geometrical structure of all the TSs located on the PES are also in consonance with the interpretation of the experimental Brønsted plots. Thus, at the rate-determining TS **TS_2** a full covalent C−N bond is formed between the nucleophilic NH_3 molecule and the carbonyl carbon atom of the β-lactam, and a positive charge is developed in the catalyst, rendering a system formally composed of NH_4^+ and amino-alcoholate interacting fragments. This formal partitioning allows a rationalization of the different TSs involved in the concerted and stepwise mechanisms. These analyses, which provide insight into the effect of ammonia as a base catalyst for either the formation of the tetrahedral intermediate or the subsequent cleavage of the β-lactam ring, may also be of interest for gaining further comprehension of amine-catalyzed cleavages of peptide bonds. A comparative analysis of the PES for the water-assisted hydrolysis and ammonia-assisted ammonolysis of azetidinones shows that these reactions follow opposite trends regarding the energetic and structural nature of their corresponding rate-determining TSs. In conclusion, the high-level Gibbs energy profiles collected in Figures 2 and 3 could be useful as a preliminary study to understand the aminolysis reaction of β-lactam antibiotics.

Acknowledgment. The authors thank CIEMAT for computer time on the Cray YMP and are grateful to both FICYT (Principado de Asturias) and DGESIC for financial support (PB-MAS96-23 and PB97-1300, respectively). N.D. also thanks FICYT for a grant (FC-97-BECA-040). In addition, D.S. thanks Professor F. J. González (The University of Oviedo) for stimulating discussions.

JO990137B